
Improvements in the Tropospheric Refraction Correction for Range Measurement [and Discussion]

Helen S. Hopfield and P. V. Angus-Leppan

Phil. Trans. R. Soc. Lond. A 1980 **294**, 341-352
doi: 10.1098/rsta.1980.0041

Email alerting service

Receive free email alerts when new articles cite this article - sign up in the box at the top right-hand corner of the article or click [here](#)

To subscribe to *Phil. Trans. R. Soc. Lond. A* go to: <http://rsta.royalsocietypublishing.org/subscriptions>

Improvements in the tropospheric refraction correction for range measurement

BY HELEN S. HOPFIELD

*The Johns Hopkins University, Applied Physics Laboratory,
Johns Hopkins Road, Laurel, Maryland 20810, U.S.A.*

The retardation of a satellite's radio signal by the Earth's troposphere and stratosphere is significant even when no bending of the signal path occurs, as in the zenith direction. The resulting error in range or Doppler data is generally estimated by assuming rectilinear propagation through a model atmosphere based on conditions at the tracking station. The two-quartic model of atmospheric refractivity that is used here ('dry' and 'wet' components) was derived earlier by the author from studies of meteorological balloon data, with parameters chosen to yield the right mean range correction at the zenith. Errors develop at very low elevation angles, partly because (a) the precise shape of the refractivity profile, involving temperature and water vapour irregularities, becomes important, and (b) signal path bending effects become significant. Corrections for the path curvature effect are presented, and possible ways of improving the profile model are discussed.

1. INTRODUCTION

Un-ionized air (the troposphere and stratosphere) has an index of refraction that is slightly greater than unity; thus it delays the passage of an electromagnetic signal travelling between a satellite and the Earth and affects range data. Since the amount of air traversed by the signal is constantly changing during a satellite pass, there is an effect on range-rate also. The effect will here be called 'tropospheric' for brevity, since 80% of it occurs below the tropopause. The ionosphere will not be discussed here.

Un-ionized air is dispersive at optical wavelengths but not in the radio region up to frequencies of approximately 30 GHz. The use of two radio frequencies therefore will not correct for the tropospheric effect. It is necessary to use either local weather measurements that include upper air data or a troposphere model adjusted for local surface conditions. A model, based on meteorological balloon data, was developed earlier to give the proper range correction at the zenith or other high elevation angles. The model involves several simplifying assumptions. The effects of two of these assumptions that cause no problem at high elevation angles will be examined here for the low-angle case: (a) that the temperature lapse rate in the troposphere is constant with height, and (b) that the bending of the signal path has a negligible effect on range.

2. BACKGROUND

The index of refraction, n , of air depends on pressure, temperature and water vapour content. A range measured through air is the integral $\int_P n ds$ taken along the signal path, which may curve, and the atmospheric effect is

$$\Delta\rho_{\text{tro}} = \int_P n ds - \rho, \quad (1)$$

[131]

where ρ is the slant range between end points of the path. If signal path bending is negligible, the integral can be taken along the slant range vector. In that case

$$\Delta\rho_{\text{tro}} = \int_V (n-1) d\rho. \quad (2)$$

The model studied here provides a value of (2) that matches the real atmosphere at the zenith and is adequate at other high elevation angles. However, at very low angles, departures of the model from the true profile of refractive index, and also signal path bending, may not be negligible, and (1) may be needed. This study examines the magnitude of these errors in the correction as the elevation angle approaches zero.

The refractivity, N ($\equiv 10^6 (n-1)$), of air is (Smith & Weintraub 1953)

$$N = 77.6 T^{-1} (P + 4810eT^{-1}), \quad (3)$$

where T is the temperature in kelvins and P and e are, respectively, the total pressure and the partial pressure of water vapour, both in millibars.† The two components of N in (3) are called the ‘dry’ and ‘wet’ components and will be subscripted d and w respectively. The N profile model used here (Hopfield 1969) is the sum of separate N_d and N_w profiles with different height parameters. Horizontal gradients in the atmosphere are assumed negligible. The fourth-degree form of the profile is theoretically justified for dry air with a normal temperature lapse rate. It is not so well justified but is not unreasonable for water vapour, and is used for convenience.

The two-quartic model of the height profile of the refractivity is:

$$\left. \begin{aligned} N &= N_d + N_w; \\ N_d &= N_{ds} (h_d - h_s)^{-4} (h_d - h)^4, \quad h \leq h_d; \\ N_w &= N_{ws} (h_w - h_s)^{-4} (h_w - h)^4, \quad h \leq h_w; \end{aligned} \right\} \quad (4)$$

where h is height above the geoid, the subscript s refers to the surface, and h_d and h_w are parameters; these were determined earlier from meteorological balloon data.

Theoretically, the height $(h_d - h_s)$ is proportional to surface temperature. In practice, it is a linear function of surface temperature:

$$h_d - h_s = (h_{d_0} - h_s) + a_{hd} T_s, \quad (5)$$

where h_{d_0} is the value of h_d at $T_s = 0^\circ\text{C}$ and a_{hd} is its temperature coefficient. The data indicate that $(h_{d_0} - h_s)$ has a value of 40.1 km worldwide, and a_{hd} is approximately 0.148 km/K. The height h_w is of the order of 10 km but varies considerably; it is treated as a constant for a given data set, since its variations are not yet well understood (Hopfield 1971, 1972, 1978).

The model N profile of (4) yields an expression for (2) that can be integrated in closed form (Hopfield 1969) at any elevation angle E of the vector ρ . The exact integral, however, is hard to compute numerically with adequate precision. A series method of evaluating it was devised by Yionoulis (1970), and a further simplification was developed by Black (1978). In any case, the resulting expression is a function of E and of surface conditions. If we assume that the atmosphere is temporarily stable and symmetrical around the observing station, we may write

$$\frac{d}{dt} (\Delta\rho_{\text{tro}}) = \frac{\partial \Delta\rho_{\text{tro}}}{\partial E} \frac{dE}{dt}. \quad (6)$$

If the value of dE/dt is known (e.g. from orbit and geometrical considerations), (6) provides the tropospheric contribution to range rate, as given by the model.

† 1 mbar = 10^2 Pa.

3. PROCEDURE FOR STUDY

The refraction contribution to range (or range-rate) computed from the present model assumes straight-line propagation through the model atmosphere and comes from (2). An actual signal travels along a curved path through a real atmosphere; to determine this effect requires the evaluation of (1). For the latter, an actual signal path was approximated by ray-tracing through an atmosphere based on meteorological balloon data. It was assumed that data from one balloon ascent represent a stable, layered atmosphere with no horizontal gradients within the region pertaining to a satellite pass. The curved path was traced by using the Snell law for spherical surfaces (Freehafer 1951). It was assumed that the ray path in each layer is an arc of a circle. The path is continuous but its radius of curvature changes at layer boundaries. The tracing procedure was iterated to reach the desired end-point. The integral was obtained by numerical integration along the curved path.

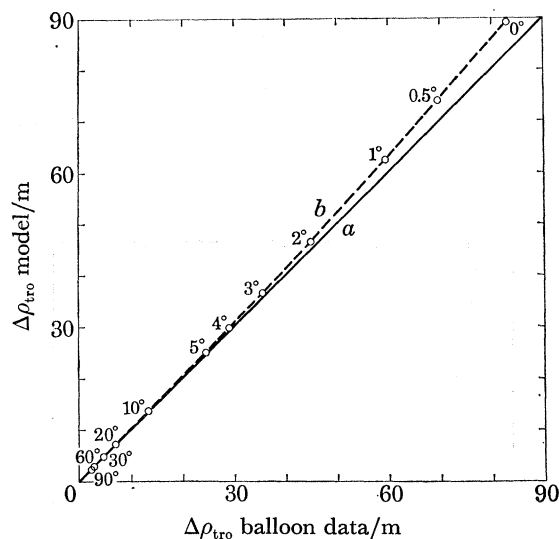


FIGURE 1. Model tropospheric effect compared with real tropospheric effect at different elevation angles (balloon data from Washington, Dulles Airport; annual mean for 1972). (a) Perfect correlation; (b) range effect given by the troposphere model.

A statistical comparison was made by using a set of observed balloon atmospheres and the corresponding set of model atmospheres (same surface refractivities). The tropospheric range effect was computed for each corresponding pair, (a) from the model, i.e. rectilinear propagation through the model atmosphere as in (2), and (b) by ray-tracing through the balloon atmosphere (equation (1)), iterating to reach an end-point at the specified elevation angle, at the desired slant range. A correlation plot of the mean results for a 1 year data set is shown in figure 1. The plotted points show the angles for which the computations were carried out. On the scale of the figure, the difference between the model and 'real' effects is perceptible only at low elevation angles, but here it can be several metres. Results are shown down to 0° elevation, but cannot be considered reliable at this point, both because of probable atmospheric irregularities near the surface and because the validity of geometric optics is questionable here.

The difference indicated in figure 1 is the mean error in the present troposphere correction. To relate this error to Doppler error, the mean effect on satellite range at 5° elevation would

change by -13 cm per degree of elevation, which is a range-rate effect of approximately -0.8 cm/s for an approaching satellite 900 km high (circular orbit, any type of pass).

The model error of figure 1 must contain both the error due to the N profile shape of the two-quartic model, and the (hitherto neglected) effect of signal path bending on range. To separate these two kinds of errors, two more computations were performed on the sets of profiles mentioned above: (*c*) curved-path propagation through the model atmospheres, and (*d*) rectilinear propagation through the balloon atmospheres, for which numerical integration was performed along a straight path. Differences between these four sets of range effects provided means of distinguishing model profile effects from path curvature effects.

For two 1 year data samples, the same four sets of range effects were determined also for the dry component of N alone. These dry component effects are approximately correct for laser signals at optical wavelengths. Comparing them with corresponding results for radio frequencies (N_{total}) helps to decide whether a model error is due to the dry or the wet component of N .

4. RESULTS

Both the profile and the path curvature effects are zero or very small at the zenith and largest at the horizon. Their mean values are shown in figure 2 for the same data sample used above. For this sample, they have the same sign. This will be discussed later.

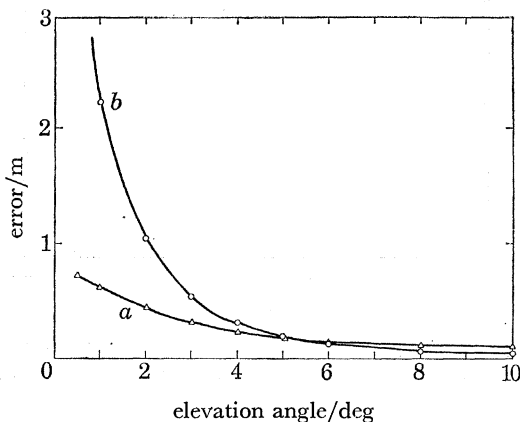


FIGURE 2. Components of error in the tropospheric correction: mean values, Washington, Dulles Airport, 1972. (*a*) Profile error effect; (*b*) path bending effect.

The two curves of figure 2 intersect, the bending effect being the larger of the two errors below 5° elevation and the smaller of the two above that. For some other data samples, the bending effect is the larger at all angles. This probably depends on local atmospheric characteristics, e.g. amount of water vapour. Both effects approach zero at the zenith.

Figures 3 and 4 show the profile and path bending effects separately: there is the same mean effect as in figure 2, with error bars showing standard deviations from the mean effect. They will now be discussed separately.

(*a*) Effects due to model profile shape

Figure 3 shows a profile-caused error in the correction model of only 0.8 m mean at the horizon, but with a standard deviation nearly twice as large as the mean. Thus the profile-

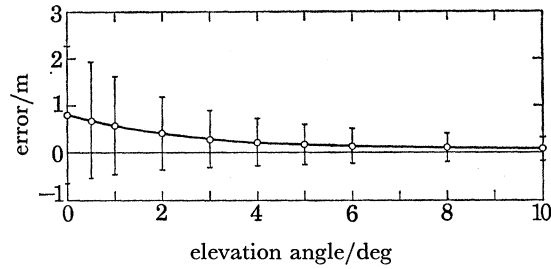


FIGURE 3. Error component due to model N profile. The difference in range effects (model minus balloon) was evaluated along a curved path; data from Washington, Dulles Airport, 1972. The error bars indicate standard deviation from the mean.

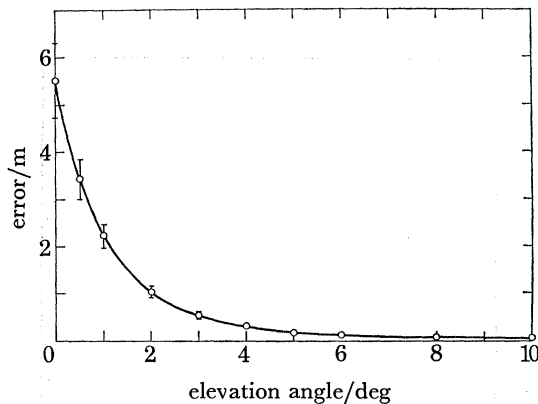


FIGURE 4. Error component due to signal path bending. The error bars indicate the standard deviation from the mean error, where this was large enough to be plotted. These values were computed from balloon data from Washington, Dulles Airport, 1972.

caused errors were predominantly, but not always, positive at very low angles (model correction too large).

When only the dry component of N was used to obtain range corrections, the profile-caused error had a slightly larger mean than for N_{total} , but a much smaller standard deviation (figure 5). This suggests that the mean error in the model is largely due to temperature irregularities while the large scatter is more an effect of water vapour. Temperature irregularities will be considered first.

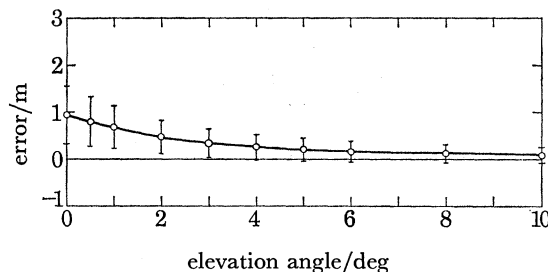


FIGURE 5. Error component due to model profile, dry part only. The difference in range effects (model minus balloon) was evaluated along a curved path; data from Washington, Dulles Airport, 1972.

(i) *Temperature irregularities*

The temperature lapse rate is crucial in determining the shape of the N_d profile (Haurwitz 1941). Equation (4) gives the shape of this profile for a lapse rate α ($\equiv -dT/dh$) of 6.8 K/km, which is a usual value in the troposphere. But the general expression is (Hopfield 1971)

$$N_d = N_{ds} (h_{d,\mu} - h_s)^{-\mu} (h_{d,\mu} - h)^\mu, \quad h \leq h_{d,\mu} \quad (7)$$

where

$$\mu = g/R\alpha - 1. \quad (8)$$

Here g is the acceleration of gravity and R is the gas constant per unit mass of dry air. This reduces to an exponential profile when $\alpha = 0$ (Bean & Thayer 1959). The parameter $h_{d,\mu}$ is the profile height that gives the proper range effect at the zenith, for the specified α and corresponding μ .

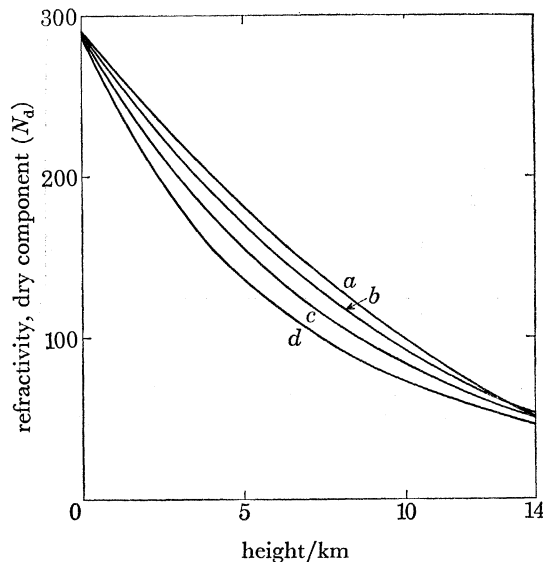


FIGURE 6. Theoretical N_d profiles of different degree μ , for different temperature lapse rates α . The surface value of N_d is 290 for all profiles. (a) $\alpha = 11.4$ K/km, $\mu = 2$; (b) $\alpha = 6.8$ K/km, $\mu = 4$; (c) $\alpha = 0$, exponential; (d) $\alpha = -11.4$ K/km, $\mu = -4$.

Figure 6 shows the lower parts of four theoretical N_d profiles corresponding to different lapse rates α ; a quartic and an exponential profile are two of them. All four would yield the same $\int N_d dh$, i.e. the same zenith range effect. In the real atmosphere, the lapse rate is often variable near the surface, although a little higher it becomes fairly constant at 6 or 7 K/km as far as the tropopause. An observed profile may include segments corresponding to several different lapse rates. It will probably deviate at some points from any simple model, but when the height parameters are chosen so that the integral $\int N_d dh$ at the zenith is correct on the average (necessary for correcting high-angle data), the sum of the deviations is zero (on the average).

Figures 7 and 8 show the lower part of sample observed profiles of temperature, N_d and N_w , for two very different temperature profiles. In figure 7 (summer), the temperature lapse rate was more nearly constant than usual: 5 K/km for the first few kilometres and 7 K/km above that. Interestingly, there was a hurricane in the region and the atmosphere must have been well mixed. The model N_d profile was in rather good agreement with the observed one.

TROPOSPHERIC REFRACTION CORRECTION FOR RANGE 347

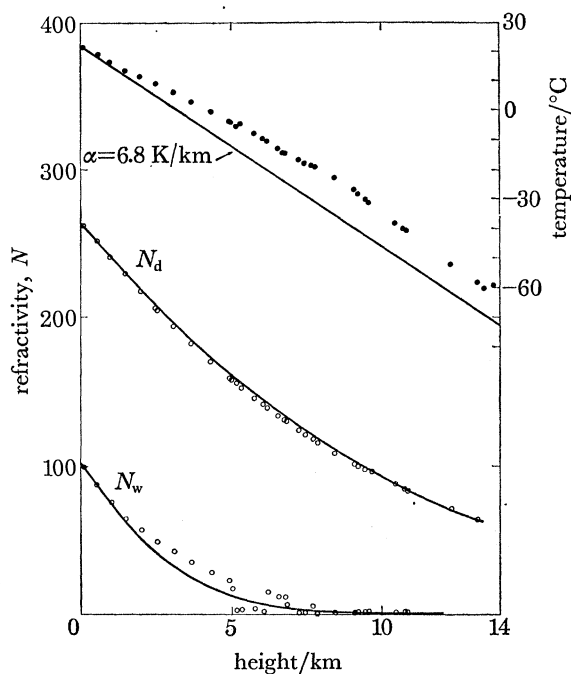


FIGURE 7. Theoretical (lines) and observed (points) profiles of temperature (●) and refractivity (○), dry (N_d) and wet (N_w) components. The data are from Washington, Dulles Airport, observed on 21 June 1972 at 00 h U.T. (7.00 p.m. local time).

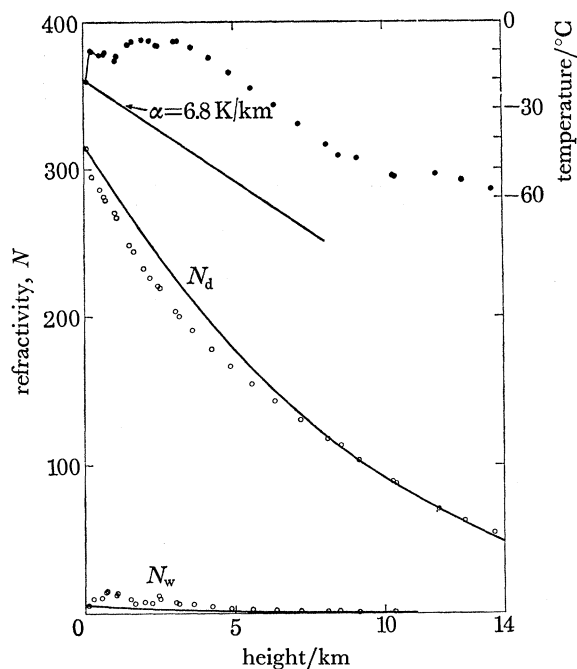


FIGURE 8. Theoretical (lines) and observed (points) profiles of temperature (●) and refractivity (○), dry (N_d) and wet (N_w) components. The data are from Washington, Dulles Airport, observed on 2 January 1968 at 12 h U.T. (7.00 a.m. local time).

Figure 8 shows the troposphere on a winter morning when there was an unusually large temperature inversion just above the surface, and a nearly constant temperature for 3 km above that. The model gives N_d values that are much too high up to 8 km, and will be too low above that, since the zenith integral $\int N_d dh$ was nearly correct for the model.

The model integral $\int N_d d\rho$ for the same atmosphere cannot be correct at the horizon.

At very low angles, the signal travels a disproportionate distance in the lowest layers of the atmosphere. Thus the integral $\int N d\rho$ is weighted toward larger values of N . This is illustrated in figure 9, which shows N_d as a function of slant range from a surface point, for four elevation angles: 90° (zenith case), 30° , 5° and 0° . The first three profiles are concave upward at all heights. The fourth is not. It can be shown mathematically that the profile of N_d against ρ has a point of inflexion at low angles. A value of $h_d = 40$ km in a quartic vertical profile gives the following result.

If

$$E > 3.7^\circ, \quad d^2 N_d / d\rho^2 > 0 \quad \text{for all } h < h_d.$$

If

$$E < 3.7^\circ, \quad d^2 N_d / d\rho^2 < 0 \quad \text{for the lower heights.}$$

The lower the elevation angle, the farther away is the point of inflexion and the larger the part of the low atmosphere that has excess weighting. (For the N_w profile, the critical angle is lower: about 2° .)

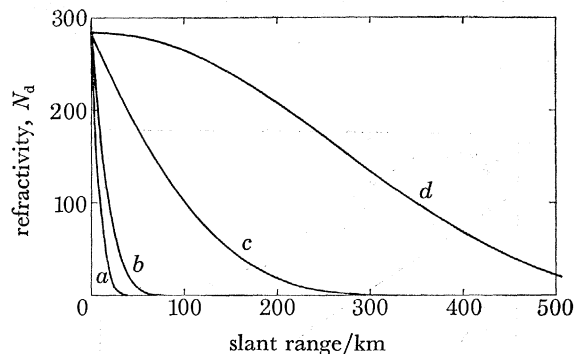


FIGURE 9. N_d profile along slant range vector at four elevation angles: (a) 90° ; (b) 30° ; (c) 5° ; (d) 0° .

If there is a systematic pattern of N_d deviations in the actual zenith profile, as in figure 8, there will be a systematic error (bias) in the dry part of the model correction at very low angles, as in figure 5.

The fact that lapse rate error can produce the observed bias has been independently established in an error analysis by Goldfinger *et al.* (1978), who used data down to 2° .

(ii) *Water vapour irregularities*

Both temperature and relative humidity profiles are important in determining the N_w profile. In figure 7 the N_w profile is smooth up to 5 km, corresponding to a smooth temperature decrease and a nearly constant relative humidity (90%). Above that height, the temperature profile was still smooth but the relative humidity profile was not. There was a dry layer (11% r.h.) from 5 to 6 km, with another humid layer above. The model prediction was too low up to

the dry layer. In figure 8, the temperature inversion and the relative humidity, which was higher above than at the surface, combined to make the observed N_w high and the model N_w much too small.

In the lower part of the troposphere, above-surface temperatures that are higher than the nominal case make the actual N_a smaller than nominal (equation 3) but the actual N_w larger than nominal, since the saturation water vapour pressure increases almost exponentially with temperature. These effects are opposite in sign, but the relative magnitudes are unpredictable because of variations in relative humidity.

Figures 3 and 5 illustrate this point. The mean model error at 0° elevation is 0.801 m for the total N profile, but 0.946 m for the dry component alone. The mean contribution of the N_w profile is therefore -0.145 m. The standard deviation of the profile error is ± 1.449 m for the total N profile but ± 0.615 m for the dry component alone. If the dry and wet component errors were uncorrelated, it could be inferred that the contribution of the N_w profile is ± 1.312 m, or more than twice as large as the dry component effect. Since some negative correlation probably exists, the contribution of the N_w profile is probably even larger.

(b) *Effects due to signal path bending*

The actual curved path of the signal is geometrically longer than a straight-line path would be, but electromagnetically shorter (the Fermat principle). Thus, neglecting path curvature makes the model prediction of tropospheric range effect too large, as shown in figure 4. The error bars indicate standard deviations for the whole 1 year data sample.

However, the bending effect can be predicted better than by a mean value, since it is a simple function of surface refractivity (Hopfield 1976). Figure 10 shows a sample of this.

Except at extremely low angles, the function is nearly linear, with a slope that is dependent on elevation angle. These relations have been formulated by Goldfinger (1978).

The bending effect increases with surface N at a slightly more than linear rate at extremely low angles (figure 10). The effect must be zero at $N_s = 0$. We have fitted an empirical curve to such data, of the form

$$\Delta\rho_{\text{curve}} = a N_s^b. \quad (9)$$

The parameters a and b were determined by a least-squares method, for a given data sample and a given elevation angle. These parameters are shown in figure 11 for a 1 year data sample.

The exponent b is approximately unity at 5 or 6° , less than 1 at high angles, and nearly 2 at 0° , but a is small at 0° . The curious behaviour of the coefficient a is found in each of the several data samples examined, and also in the corresponding model atmosphere samples. It has not been quantitatively explained. However, it must be related to the curvature of the Earth, the effect of which was illustrated in the low-angle distortion of the N profile shape. In figure 9, the transformation between the high-angle and low-angle forms of the N profile would occur between 3 and 4° elevation. In every case examined, the maximum of the a curve also occurs in that interval. The radius of the Earth is a basic parameter in the ray-tracing procedure, and the curvatures of the Earth and of the atmospheric layers are clearly among the most important parameters in determining the curvature of the signal path.

The values found for a and b of (9) differ somewhat for different samples, but it appears probable that a standard set of a and b values can be found that will be adequate for a variety of atmospheres.

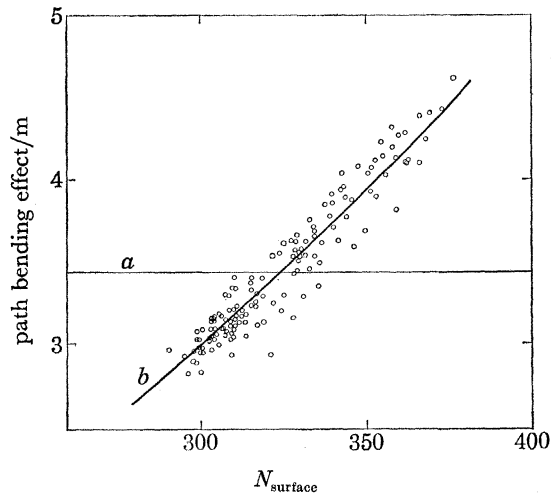


FIGURE 10. Path bending effect on range for N profiles observed at Washington, Dulles Airport, 1972. The plotted points represent individual balloon flights and are a random sampling from the entire year. (a) This line represents the mean, 3.440 m, for the year; (b) this curve is the line $\Delta\rho_{\text{curve}} = a N_s^b$ with $a = 1.1682 \times 10^{-4}$ m, $b = 1.77926$.

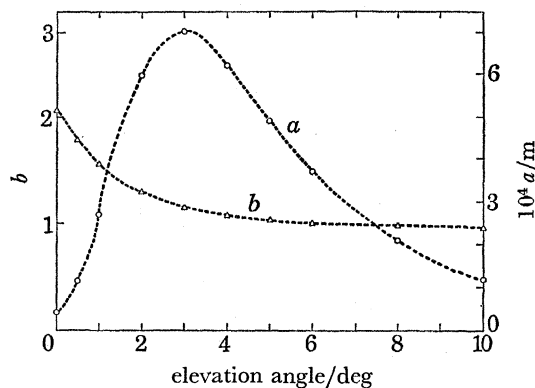


FIGURE 11. Parameters for bending effect on range, for the equation $\Delta\rho_{\text{curve}} = a N_s^b$: (a) coefficient a ; (b) exponent b . These parameters were determined from balloon data for the year 1972, observed at Washington, Dulles Airport.

By using (9) with suitable parameters, or the expressions of Goldfinger (1978), the neglected path curvature effect for a balloon atmosphere can be predicted from N_s with a fraction of the error shown in figure 4. For obvious reasons, the prediction is still more precise for a model atmosphere: an r.m.s. deviation of not more than ± 2 cm down to the horizon.

5. DISCUSSION AND CONCLUSIONS

The results shown in these figures pertain mostly to a single 1 year set of balloon data: two balloons per day for the year 1972, launched near Dulles Airport, Washington, D.C., U.S.A. (data from the U.S. National Climatic Center). Comparisons can therefore be made between the figures. However, all the same computations were carried out for a second 1 year set of data (1971) from the same location, and for the same 2 years for Ocean Weather Ship E in the mid-Atlantic (35° N, 48° W). Partial computations were also performed for many other samples. The numerical results, of course, varied somewhat, but the kinds of results were all in agreement.

Two obvious improvements to be made in the present tropospheric range correction are a correction for signal path bending, and an improvement of the model N profile shape. These can be taken in either order, but it is preferable to make the path bending correction first, as will be discussed below.

As to the path bending correction, we have as yet no theoretical expressions for the parameters a and b of (9), but empirical parameters are now available for specific angles, for several kinds of atmospheric samples. These can be the basis for interpolation at other elevation angles. This procedure can doubtless be improved later, but should yield a good first order approximation to the path bending correction.

As regards N profile improvement, we found above that the same temperature deviation in the lower troposphere can both make the N_d correction too large and the N_w correction too small at low angles. Such error components were found in the mean correction. It is not yet known whether the same change in the model profile will yield the right mean magnitudes for these two effects.

The temperature lapse rate of 6.8 K/km that corresponds to our theoretical N_d profile is fairly near the correct one above the surface layers of air, but is likely to be too large near the surface. This 'surface' irregularity varies in extent but may go as high as 5 or 6 km.

It may be desirable to postulate a 'surface' layer of higher degree than four (e.g. degree eight, or even exponential), at least for the N_d profile, with the quartic form continuing above this layer. The change for N_w might have to be different. This has not yet been tried. The parameters for such a profile could be obtained from meteorological balloon data, as were the parameters for the present model. It is hoped that both the thickness of the 'surface' layer and the degree of profile to be used (equation 7) could be determined in this way. It may be desirable to take into account seasonal or even diurnal effects.

The addition of a microwave radiometer to the station instrumentation could contribute materially to determining the temperature profile and the water vapour content along the line of sight. A great deal of work is being done along this line; the two references quoted are only a small sample (Wark 1970; Staelin *et al.* 1976).

An alternative approach would be to determine the necessary parameters from satellite tracking data, so that the tracking data could become in a sense 'self-correcting'. Early attempts to do this without first correcting for path bending have not been completely satisfactory (Arie Eisner, unpublished report). The path bending effect should be corrected first, since it is larger than the profile error effect at angles below 5° , and data at very low angles carry most of the refraction information. We need to learn to ask the right questions of the low-angle data.

If tracking data can provide the refraction correction, it can be hoped that such data can also, in the future, provide useful weather information.

Helpful discussions with Mr H. D. Black and the collaboration of Mr H. K. Utterback in the computer programming and computations are very gratefully acknowledged.

This work was supported by the U.S. Department of the Navy under Contract N00024-78-C-5384 with The Johns Hopkins University Applied Physics Laboratory.

REFERENCES (Hopfield)

- Bean, B. R. & Thayer, G. D. 1959 *CRPL exponential reference atmosphere*. U.S. National Bureau of Standards, Monograph 4.
- Black, H. D. 1978 An easily implemented algorithm for the tropospheric range correction. *J. geophys. Res.* B **83**, 1825–1828.
- Freehafer, J. E. 1951 Geometrical optics. In *Propagation of short radio waves* (ed. D. E. Kerr), vol. 13, chap. 2. New York: McGraw-Hill.
- Goldfinger, A. D., Black, H. D., Bush, G. B., Ebert, W. L., Foner, S. N., Hart, R. W. & Katz, I. 1978 A satellite system for measuring atmospheric surface pressure. *JHU/APL Internal Report* no. SDO 5077, section 3.
- Haurwitz, B. 1941 *Dynamic meteorology*, pp. 11–22. New York: McGraw-Hill.
- Hopfield, H. S. 1969 Two-quartic tropospheric refractivity profile for correcting satellite data. *J. geophys. Res.* **74**, 4487–4499.
- Hopfield, H. S. 1971 Tropospheric effect on electromagnetically measured range: Prediction from surface weather data. *Radio Sci.* **6**, 357–367.
- Hopfield, H. S. 1972 Tropospheric range error parameters: further studies. *JHU/APL Report* no. CP 015.
- Hopfield, H. S. 1976 Tropospheric effects on signals at very low elevation angles. *JHU/APL Report* no. TG 1291.
- Hopfield, H. S. 1978 Tropospheric correction of electromagnetic ranging signals to a satellite: study of parameters. In *Proceedings of the International Symposium on Electromagnetic Distance Measurement and the Influence of Atmospheric Refraction*, Wageningen, The Netherlands, May 1977 (ed. P. Richardus), pp. 205–215.
- Smith, Jr, E. K. & Weintraub, S. 1953 The constants in the equation for atmospheric refractive index at radio frequencies. *Proc. Inst. Radio Engrs* **41**, 1035–1037.
- Staelin, D. H., Kunzi, K. F., Pettyjohn, R. L., Poon, R. K. L., Wilcox, R. W. & Waters, J. W. 1976 Remote sensing of atmospheric water vapor and liquid water with the Nimbus 5 microwave spectrometer. *J. appl. Met.* **15**, 1204–1214.
- Wark, D. Q. 1970 SIRS: An experiment to measure the free air temperature from a satellite. *Appl. Opt.* **9**, 1761–1766.
- Yionoulis, S. M. 1970 Algorithm to compute tropospheric effects on range measurements. *J. geophys. Res.* **75**, 36, 7636–7637.

Discussion

P. V. ANGUS-LEPPAN (*University of New South Wales, Australia*). In the lowest levels of the atmosphere, where the meteorological measurements are made, there are large daily variations and random variations. At what time of day were the balloon ascents, used in your analysis, made? Does Mrs Hopfield see progress through applying corrections to the temperature and pressure values, taken at the surface, to make them more representative of the higher atmospheric layers?

HELEN S. HOPFIELD. The balloon ascents used in our analysis were all made at 00 h and 12 h Universal time. The ascents at Dulles Airport, near Washington, D.C., U.S.A., were therefore made at 7.00 a.m. and 7.00 p.m. local standard time.

Discrepancies from a nominal profile are much smaller for the total pressure than for temperature and water vapour content. The latter two (which are somewhat correlated) need corrections that, as yet, we do not have. Directional radiometers at the tracking site (looking along the instantaneous line-of-sight to the satellite) may be useful here, in the future.